

Absolute cross sections for electronimpact ionization and dissociative ionization of the SiF free radical

Todd R. Hayes, Robert C. Wetzel, Frank A. Baiocchi, and Robert S. Freund

Citation: *The Journal of Chemical Physics* **88**, 823 (1988); doi: 10.1063/1.454161

View online: <http://dx.doi.org/10.1063/1.454161>

View Table of Contents: <http://scitation.aip.org/content/aip/journal/jcp/88/2?ver=pdfcov>

Published by the [AIP Publishing](#)

Articles you may be interested in

[Absolute electron-impact total ionization cross sections of chlorofluoromethanes](#)

J. Chem. Phys. **121**, 11653 (2004); 10.1063/1.1808413

[Comment on the accuracy of absolute electron-impact ionization cross sections for molecules](#)

J. Chem. Phys. **114**, 4741 (2001); 10.1063/1.1346641

[Electron-impact ionization cross sections for polyatomic molecules, radicals, and ions](#)

AIP Conf. Proc. **543**, 220 (2000); 10.1063/1.1336281

[Absolute cross sections for the electron impact ionization of the NF₂ and NF free radicals](#)

J. Chem. Phys. **100**, 5626 (1994); 10.1063/1.467129

[Electronimpact ionization cross sections of the SiF₃ free radical](#)

J. Chem. Phys. **89**, 4035 (1988); 10.1063/1.454836



Absolute cross sections for electron-impact ionization and dissociative ionization of the SiF free radical

Todd R. Hayes, Robert C. Wetzell, Frank A. Baiocchi, and Robert S. Freund
AT&T Bell Laboratories, Murray Hill, New Jersey 07974

(Received 29 May 1987; accepted 16 September 1987)

Absolute cross sections for electron-impact ionization of the SiF free radical from threshold to 200 eV are presented for formation of the parent SiF⁺ ion and the fragment Si⁺ and F⁺ ions. A fast beam of SiF is prepared by charge transfer neutralization of an SiF⁺ beam. The radicals form in the ground electronic state and predominantly in their ground vibrational state, as shown by agreement of the measured ionization threshold with the ionization potential. The absolute cross section for SiF → SiF⁺ at 70 eV is $3.90 \pm 0.32 \text{ \AA}^2$. The ratio of cross sections for formation of Si⁺ to that for SiF⁺ at 70 eV is 0.528 ± 0.024 ; the ratio for formation of F⁺ to that of SiF⁺ is 0.060 ± 0.008 . The observed threshold energy for Si⁺ formation indicates the importance of ion pair formation SiF → Si⁺ + F⁻. Breaks in the cross section at 14.3 and 17 eV are assigned as dissociative ionization thresholds.

I. INTRODUCTION

Free radicals are important components of the gas discharge environment, yet little is known about electron-impact ionization and dissociative ionization of these reactive species. The dearth of data is due to difficulties in preparation and handling as well as the difficulty of quantitatively collecting the dissociation fragments. Using a fast neutral beam technique which minimizes both of these problems, we have obtained the first absolute electron-impact ionization cross section measurements of the SiF radical. In addition to our preliminary report¹ on the ionization of CD₂ and CD₃, the only other data published on free radical ionization cross sections is a report of the fragmentation pattern of SiF₂ at 30 eV.²

The SiF_x radicals are known or are suspected to be products of the etching of Si by fluorinated gases. SiF₂, for example, has been detected both by mass spectrometry² and laser induced fluorescence³ as a volatile product in the spontaneous etching of Si by XeF₂ and F atoms. When fluorine-containing plasmas are used to etch Si, the radicals are present as products of both spontaneous and ion impact-induced desorption, as well as from dissociation of etch-produced SiF₄ in the discharge. SiF, for example, has been detected by laser induced fluorescence above a Si surface in a CF₄ plasma,⁴ but residence time studies indicated that the source of the radical was primarily SiF₄ dissociated by the plasma.

Ionization cross section measurements of the SiF_x radicals are necessary for mass spectrometric studies of etching, in that accurate ionic fragmentation patterns permit calculation of the relative abundances of the volatile fluorinated silicon products. In addition, quantitative modeling of gas discharges requires accurate experimental determinations or theoretical estimates of ionization and dissociative ionization cross sections.

In this paper we present absolute measurements of the electron impact ionization cross sections for the processes SiF + e⁻ → SiF⁺, Si⁺, F⁺ from threshold to 200 eV. The charge transfer step used to produce the fast neutral beam and the internal energy of the radical beams are discussed in

the context of the electronic states of SiF and SiF⁺. The threshold regions of the product ions and thermochemical data are used to assign probable ion production mechanisms.

II. EXPERIMENTAL

A. Apparatus and dissociative ionization

The apparatus has been described and evaluated in a study of the ionization of the rare gas atoms.⁵ Here we briefly discuss the apparatus and concentrate only on those additional design features which are essential for accurate measurements of cross sections for the production of fragment ions from molecular species.

A diagram of the apparatus is shown in Fig. 1. The precursor ion beam is generated by extracting ions from a dc discharge (Coultron source), accelerating them to a few keV, and velocity filtering the beam to select the ion of interest. A discharge through SiF₄ is used to obtain SiF⁺. Fast, neutral SiF radicals are created by passing the ion beam through a region of higher pressure (approximately 0.1 mTorr Xe) in which charge transfer neutralization takes place with an efficiency of about 0.1%. The neutral beam then passes through a beam-defining aperture, crosses the electron beam, and is ultimately monitored by measuring the secondary electron current generated when the fast beam hits a Nichrome surface.

Electron-impact ionization of the radical beam in the electron gun creates an ion beam which is comprised of parent ions and dissociatively produced fragment ions. The parent ion beam retains its initial collimation and energy spread because momentum transfer to the ion from the electron collision is negligible. Fragment ions, however, are born with kinetic energy distributions which significantly increase the energy spread of the fragment beams as well as disperse it away from the beam axis. The kinematics of the dissociation process is demonstrated in the Newton diagram in Fig. 2. Consider a parent molecule of mass M_p and initial velocity \bar{V} which dissociates to give fragments of mass m_1 and m_2 , where the subscript 2 denotes the ionic fragment.

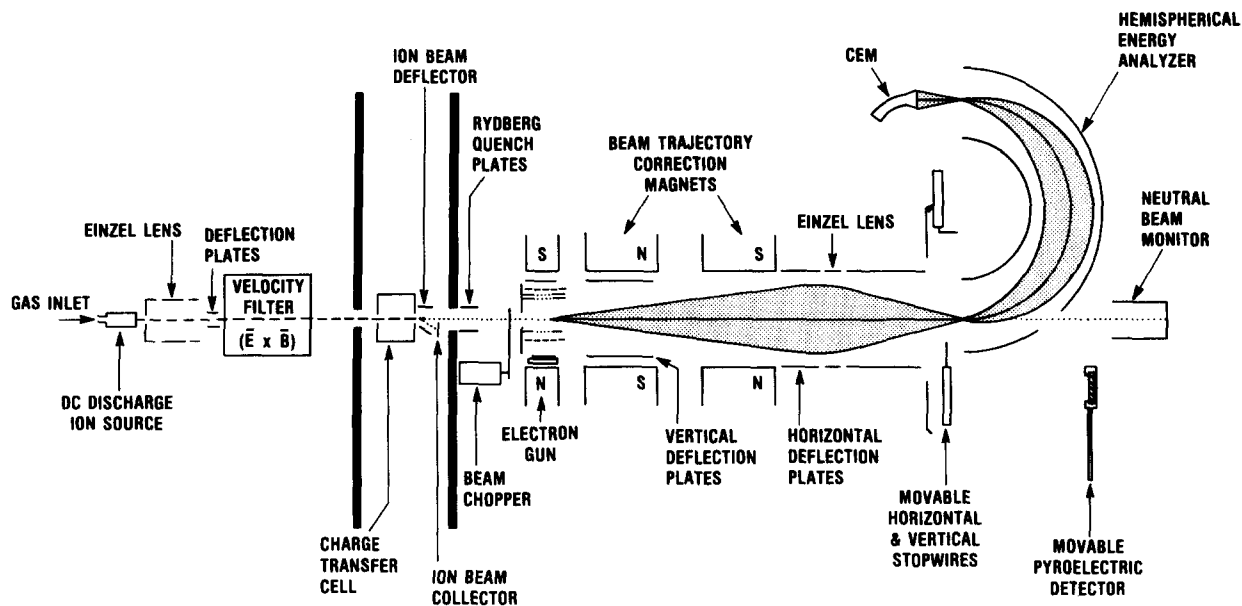


FIG. 1. Side view of the apparatus. For clarity, the hemispherical energy analyzer is shown above the beam axis, a rotation of 90° from its actual horizontal position.

The two fragments possess velocities \bar{U}_1 and \bar{U}_2 in the center of mass reference frame, and \bar{V}_1 and \bar{V}_2 in the lab frame. Although θ may vary from $0 < \theta < 360^\circ$ for any individual event, we consider the case of $\theta = 90^\circ$, which results in the largest angular spread in the beam (χ_2).

For a parent molecule of initial kinetic energy E_p and fragment energy ϵ_2 associated with the process, $\tan \chi_2 = (\epsilon_2 M_p / E_p m_2)^{1/2} \approx \chi_2$ (rad) for small angles of χ_2 . Thus χ_2 decreases with increasing beam kinetic energy. Of course there is a distribution of ϵ_2 's and θ 's for any dissociation process, so there is also an angular distribution of the fragment ion beam.

This analysis illustrates the advantage of using higher beam energies in order to collect 100% of the fragment ions. In practice, while higher beam energies result in more complete collection, background ion fluxes due to collisional ionization also increase with energy, and we find 4000 eV to be a practical upper limit at our present background pressure of approximately 5×10^{-8} Torr along the beam path. Most cross section measurements are made at 3000 eV, a good compromise between maximum collection and signal-to-background levels.

The diverging fragment ion beam is focused at the entrance of the hemispherical energy analyzer. This is per-

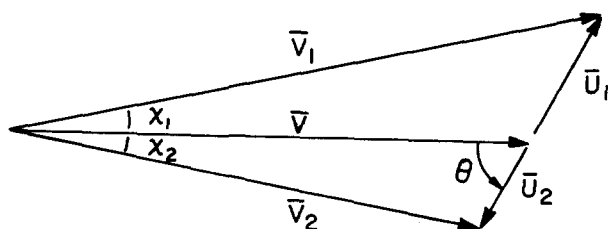


FIG. 2. Kinematics of dissociation of a fast molecule into a neutral fragment (1) and an ionic fragment (2).

formed by a three-element einzel lens, which is located at about two-thirds of the distance from the collision region to the entrance of the hemispherical analyzer (Fig. 1). A voltage equal to 80%–90% of the beam energy is applied to the center element of the lens, the front and back elements being held at ground potential. The hemispherical energy analyzer separates parent and fragment ions by their energy (or mass-to-charge ratio), allowing separate measurement of the intensity of each ion and yielding partial cross section values. (Note that for clarity, the hemispherical analyzer is shown rotated 90° from its actual horizontal position.) Mass interference is not a problem, because the mass differences between SiF^+ , Si^+ , and F^+ are greater than the energy resolution of the analyzer. The analyzer affords two-dimensional radial and azimuthal focusing while dispersing ions of different energies in the radial direction. Neglecting energy of dissociation, the fragment possesses the same velocity as the parent, and so its kinetic energy is $E_2 = E_p m_2 / M_p$.

Ions are detected by a channeltron electron multiplier (CEM)⁶ with a 2.54 cm diameter entrance cone, positioned two centimeters from the exit of the hemispherical analyzer. Ion spatial distributions are measured via two movable 0.25 cm wide slits oriented perpendicular to one another and positioned just in front of the CEM. The spatial distributions of SiF^+ and Si^+ on the CEM are shown in Fig. 3. The width of an ion distribution in the azimuthal direction is due to the size of the interaction region, to focusing aberrations, and to the angular spread of the fragment ion beam. In the radial direction the width results from the above factors plus dispersion due to the energy spread of the beam.

The SiF^+ distribution is found to be relatively narrow in both directions, indicating that the beam is well collimated and has a narrow energy spread. The Si^+ fragment beam has both a greater angular divergence and energy spread than the parent ion, consistent with its production by dissociation.

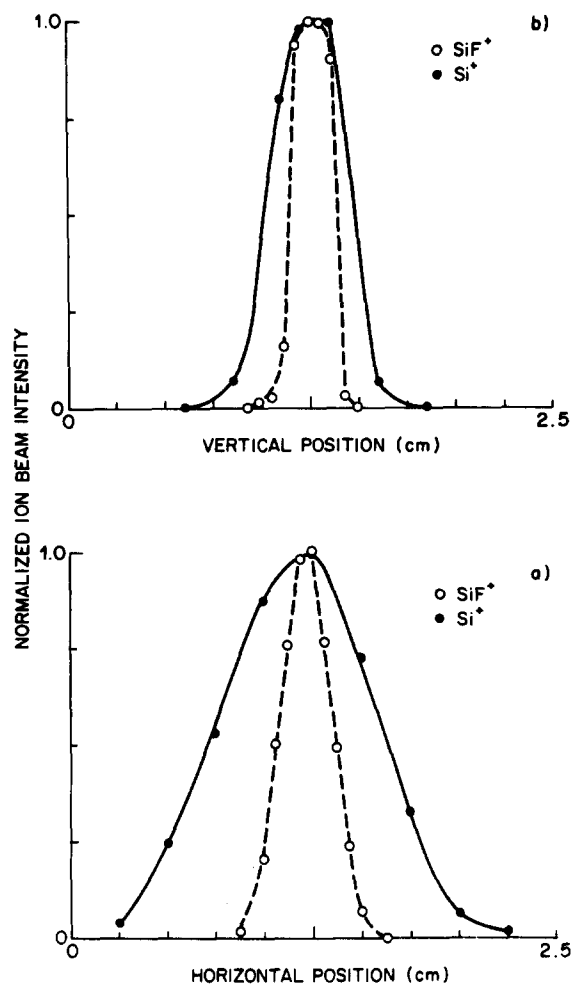


FIG. 3. Spatial distributions of SiF⁺ and Si⁺ from SiF at the CEM.

The maximum scattering angle χ_{\max} for the production of fragment Si⁺ can be roughly calculated using the data in Fig. 3(a) and the distances between the CEM, hemispherical analyzer, einzel lens, and electron gun. The result, $\chi_{\max} = 4.1^\circ$, corresponds to a reasonable maximum dissociation energy ϵ_2 of 9.2 eV.

Figure 3 demonstrates that both the SiF⁺ and Si⁺ ion beams fall completely within the 2.5 cm diameter of the CEM entrance cone. When, however, the mass of the fragment ion is small compared to that of the parent (e.g., F⁺ from SiF⁺) the energy spread in the fragment beam may be so great that less than 100% of the ion beam is detected at the CEM. In this case, we can measure the approximate beam profile by centering the vertical slit on the CEM and scanning the voltage of the hemispherical analyzer such that the beam is swept across the slit. This yields an ion intensity vs voltage plot whose voltage axis can be calibrated in terms of the CEM edges. The collection fraction K for a beam centered on the CEM is then determined by taking the ratio of the area within the CEM boundaries to the total beam area. Although the method is not perfect due to the finite slit width, the possible loss of some ions above and below the CEM, and the fact that the centered and scanned beams take slightly different paths through the analyzer, it provides a

useful estimate of the fraction collected which we believe is accurate to $\pm 10\%$.

B. Calibration of electron energy scale

Since we cannot be certain of the electronic and vibrational states of the SiF beam, we cannot use the spectroscopic ionization potential to calibrate the electron energy scale. Experience has shown that the voltage applied between the cathode and the collision region is about 2 or 3 V greater than the energy of the electrons in the collision region. This is due to two sources, the contact potential difference between the barium–strontium oxide cathode and the molybdenum plates of the collision region, and the potential depression caused by electron space charge.

We expect the contact potential to be independent of electron energy. The space charge depression of the potential, however, is expected⁷ to be equal (in V) to $V_{sc} = 0.015I_e (\mu\text{A})/E_c^{1/2}$, where E_c is the corrected threshold energy (in eV). Thus, E_c is given in terms of the measured threshold energy E_m by

$$E_c = E_m - V_{cp} - V_{sc}. \quad (1)$$

We find that with $V_{cp} = 1.0$ eV, Eq. (1) corrects over a dozen measurements of the reference ionization potentials of Ga (6.00 eV) and Xe (12.13 eV) to within 0.3 eV.

C. Internal energy of the SiF radical

Charge transfer neutralization of a molecular ion does not necessarily produce the neutral molecule in a well-defined state. Thus, it is important to characterize the neutral beam, so that subsequent ionization measurements are meaningful. In this work, we aim to produce the beam in the ground electronic and vibrational states. (In the future, it would be valuable to obtain cross section data for ionization of vibrationally or electronically excited molecules.) We use energy resonance as a guide in selecting the gas to use for charge transfer, although for 3 keV collisions, the unknown Franck–Condon factors between the ion and the neutral may be even more important in determining the vibrational energy of the neutral molecule.⁸

It is difficult to find a gas to resonantly neutralize the ground $X^1\Sigma^+$ state of SiF⁺ because it lies only 7.26 eV above the ground state of neutral SiF,⁹ and few high-vapor-pressure gases have such a low ionization potential. Instead, we neutralize the metastable $a^3\Pi$ state of SiF⁺, which apparently has a significant population in our ion beam. Although its electronic excitation energy is unknown, we estimate by analogy with isoelectronic SiO and AlF¹⁰ that it lies between 3.4 and 4.2 eV above the SiF⁺ ground state and therefore about 10.7 to 11.5 eV above the SiF ground state. Charge transfer with xenon, which has a 12.1 eV ionization potential, is therefore only about 1 eV off-resonant, and in practice we find that it produces a sufficiently intense neutral beam. Figure 4 shows the appropriate energy levels.

Charge transfer takes place entirely to the ground electronic state of SiF; we find no experimental evidence of electronically excited SiF radicals in the beam, which should reveal themselves by lowering the ionization threshold. Our measured ionization potential (Fig. 5) is 7.4 ± 0.1 eV, in

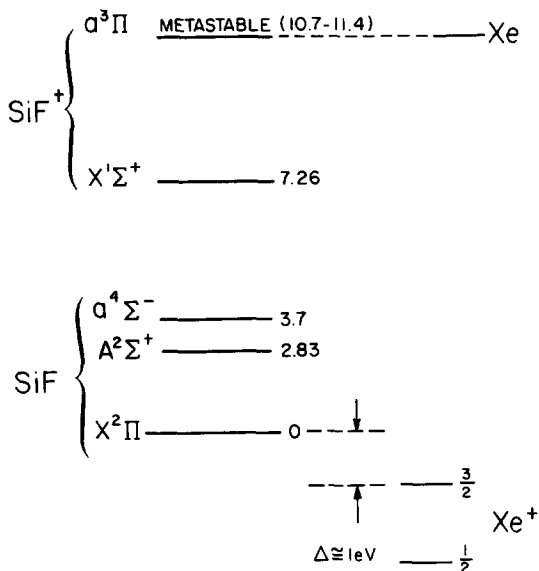


FIG. 4 Potential energy diagram for charge transfer from Xe to SiF⁺.

good agreement with the 7.26 eV spectroscopic ionization potential.⁹ This indicates that only X²Π SiF is present in the beam. The first excited state of SiF at 2.8 eV would have a much lower ionization threshold, and in addition it has a lifetime of 0.23 μs,¹¹ which is much shorter than the 2 μs time-of-flight from the charge transfer cell to the electron gun. Although the second excited state is metastable, it lies at 3.7 eV and would be easily discernable by its lower threshold. Similarly, if any higher electronic state were populated significantly, the ionization threshold would be lowered by an easily observable amount.

Vibrational excitation of the X²Π state also would lead to a lowered threshold. Knowledge of the Franck–Condon factors, or at least the excited ion state internuclear distance, would help predict the amount of vibrational excitation to be

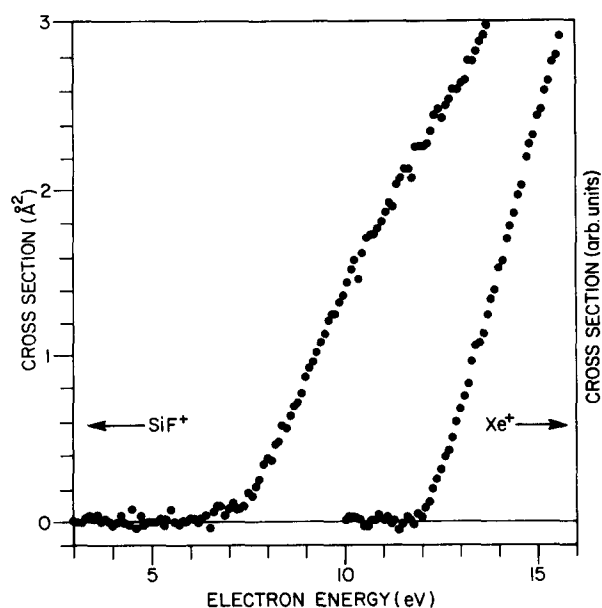


FIG. 5. Absolute electron impact ionization cross section for SiF + e⁻ → SiF⁺ + 2e⁻ in the threshold region, and the xenon relative ionization threshold used to calibrate the electron energy scale.

expected, but no such data are available. Our measurement of the SiF → SiF⁺ threshold (Fig. 5), although of too poor signal-to-noise to be definitive, reveals a small foot extending at most 1 eV below the principal SiF⁺ threshold, indicating that no more than a small fraction of the SiF is vibrationally excited. We conclude that SiF⁺ charge transfer with Xe produces a nominally ground state SiF beam.

D. Measurement procedures

The absolute cross section of the SiF⁺ parent ion at an electron energy of 70 eV was determined by measuring or carefully estimating each of the terms in the working expression for the cross section:⁵

$$\sigma(\text{cm}^2) = \frac{1.952 \times 10^{-30} C_{\text{corr}} \gamma T}{I_{\text{sec}} K \epsilon F M^{1/2} I_e (1 + 1.60\eta)}. \quad (2)$$

C_{corr} is the ion count rate corrected for the counting system deadtime and I_e is the electron current. The neutral flux $I_{\text{sec}}/\gamma T$ is given by the secondary electron current generated by the neutral beam. F is a geometric factor which describes the overlap between the electron and neutral beams, K is the fraction of the ion beam collected, and M is the molecular weight of the parent radical (atomic units). The two remaining factors, ϵ (the CEM detection efficiency) and $(1 + 1.60\eta)$, a factor accounting for electron reflection within the electron gun, are not directly measured but have been carefully estimated.

Fragment ion cross sections were determined from the ratio of the “normalized” ion signals $I_{\text{norm}} = C_{\text{corr}}/I_{\text{sec}} I_e$ for both the fragment and parent ions, corrected by the collection fraction for each ion:

$$\frac{\sigma_{\text{fragment}}}{\sigma_{\text{parent}}} = \frac{K_p I_{\text{norm},f}}{K_f I_{\text{norm},p}}. \quad (3)$$

Here we assume equal CEM detection efficiencies for the parent and fragment ions. We believe this to be reasonable, since no variation in detection efficiency was found for the rare gas ions⁵ which have widely differing potential energies, masses and velocities. Note that $K_{\text{parent}} = 1.0$ and $K_{\text{fragment}} < 1.0$ depending on fragment ion dispersion at the CEM. Ratios reported here were measured at an electron energy of 70 eV.

It is possible that the fraction of fragment ions collected may vary with electron energy, if collisions with more energetic electrons lead to fragment ions with higher kinetic energy. This effect was examined for the Si⁺ fragment by comparing K values obtained at low, intermediate and high electron energies. K was found to be independent of electron energy.

E. Background from Si Rydberg atoms

The SiF radical beam was found to contain small quantities of Si Rydberg atoms which arise via collisions between the SiF⁺ beam and background or charge transfer gases. Those with principal quantum number $n > 19$ are field ionized by the Rydberg quench plates and those with $n \lesssim 8$ radiate in a time shorter than their time-of-flight to the electron gun. Those with $9 < n < 19$ survive. As a result of the very large electron impact ionization cross sections for such

species¹² (on the order of $n^4 \text{Å}^2$) the Si^+ signals detected from Rydberg atom ionization in the electron beam were under certain conditions comparable to the Si^+ signal detected from dissociative ionization of SiF. Si Rydberg atoms in the beam are identified by an Si^+ signal which maximizes at very low electron energy ($\ll 1$ eV) and decays approximately as $\ln E/E \cdot I_{\text{norm}}$ was corrected for Rydberg signals by applying the Rydberg atom correction technique described in Ref. 5, so the absolute cross section at 70 eV for the processes $\text{SiF} + e^- \rightarrow \text{Si}^+$ has been corrected for this background. The 0 to 200 eV cross section curves were corrected by subtracting from the data a function of the form $\alpha \ln E/E$, where α is a scaling constant chosen to best fit the measured Rydberg contribution at 70 eV and the data below the appearance potential for Si^+ , which is due only to ionization of Rydberg atoms.

III. RESULTS

Measurements were made for the production of the singly charged SiF^+ , Si^+ , and F^+ ions from electron impact ionization of SiF. Double ionization was too weak to be investigated.

Cross section shapes for SiF^+ , Si^+ , and F^+ were measured from 0 to 200 eV electron energy at electron energy intervals which vary from 0.125 eV in the threshold region, to 5 eV at higher energies where lower data density is sufficient. Repetitive scans were added from 1 to 8 h, depending on the signal-to-noise level. Next, the parent ion shape was normalized to the absolute cross section at 70 eV. Then the fragment ion shapes were normalized using the fragment-to-parent ion ratios. Results are given in Table I and in Fig. 6. Ratios measured at a variety of energies confirmed the shapes measured as above. The small shape correction function of Eq. (15) in Ref. 5 corrects for systematic errors in our electron gun. The cross section for parent ionization $\text{SiF} \rightarrow \text{SiF}^+$ was found to rise linearly for about 5 eV above its threshold at 7.4 ± 0.1 eV to peak at approximately 28 eV, and then to decrease monotonically. The cross section of Si^+ formation peaks at about 50 eV and then decreases slowly. In each case, the peak lies at approximately four times the threshold energy, as predicted by classical and semi-empirical approximations.¹³

Table II contains the measured absolute cross section and ratio values at 70 eV, and their random uncertainties (one standard deviation). For this apparatus, the systematic uncertainty of the absolute cross section measurement has been determined⁵ to be $\pm 12\%$. Combining the random and systematic uncertainties in quadrature gives an overall uncertainty of $\pm 15\%$ for the absolute cross section measurement. The systematic uncertainty of the ratio measurements is much lower than that of the absolute measurements because many sources of error cancel in the ratio. Thus the overall uncertainty of the Si^+/SiF^+ ratio is dominated by its $\pm 5\%$ random uncertainty. The F^+/SiF^+ ratio, although corrected for incomplete collection, is believed to be a lower limit, since it is possible that some F^+ fragments with high dissociative energy may have been lost before the CEM. We estimate it to be low by no more than 10% with a random uncertainty of $\pm 13\%$.

TABLE I. Cross sections for electron impact ionization of SiF.

Electron energy (eV)	Product ion cross section (Å^2)		
	SiF^+	Si^+	F^+
5	0.03		
6	0.05		
7	0.16		
8	0.47	0.01	
9	0.96	0.00	
10	1.55	0.02	
11	2.10	0.05	
12	2.59	0.10	
13	3.05	0.15	
14	3.39	0.19	
15	3.65	0.26	
16	3.88	0.37	
17	4.08	0.49	
18	4.19	0.61	
19	4.16	0.77	
20	4.24	0.93	0.07
21	4.36	1.10	0.08
22	4.31	1.24	0.03
23	4.21	1.40	0.01
24	4.34	1.46	0.05
25	4.35	1.51	0.06
26	4.41	1.56	0.06
27	4.43	1.65	0.07
28	4.39	1.69	0.06
29	4.41	1.73	0.09
30	4.33	1.79	0.05
32	4.43	1.85	0.08
34	4.41	1.87	0.11
36	4.36	1.95	0.15
38	4.26	1.95	0.17
40	4.23	2.01	0.15
45	4.20	2.04	0.20
50	4.18	2.06	0.20
55	4.11	2.11	0.19
60	4.10	2.07	0.19
65	3.96	2.07	0.22
70	3.90	2.06	0.24
75	3.84	2.04	0.24
80	3.75	2.02	0.25
85	3.62	2.03	0.20
90	3.56	2.03	0.21
95	3.57	2.05	0.23
100	3.51	2.04	0.27
105	3.43	2.01	0.27
110	3.35	1.97	0.24
115	3.34	1.92	0.24
120	3.32	1.91	0.23
125	3.32	1.93	0.23
130	3.26	1.92	0.20
135	3.16	1.89	0.21
140	3.11	1.86	0.21
145	3.08	1.83	0.23
150	3.01	1.79	0.23
155	2.99	1.80	0.21
160	2.97	1.79	0.22
165	2.91	1.76	0.23
170	2.86	1.74	0.19
175	2.81	1.74	0.20
180	2.73	1.74	0.23
185	2.69	1.68	0.20
190	2.68	1.61	0.20
195	2.63	1.60	0.20
200	2.58	1.62	0.13

The relative ion abundance or cracking pattern of SiF at 70 eV (from Table II) is 100:53:6 ($\text{SiF}^+:\text{Si}^+:\text{F}^+$). This is the absolute cracking pattern with complete collection of all

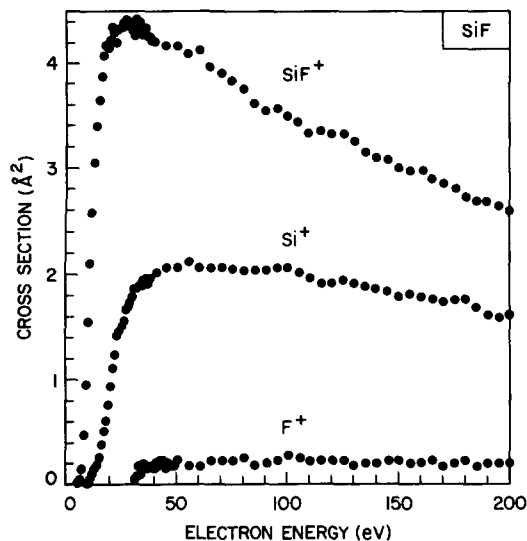


FIG. 6. Electron impact ionization cross sections vs energy from threshold to 200 eV for $\text{SiF} + e^- \rightarrow \text{SiF}^+, \text{Si}^+, \text{and } \text{F}^+$.

fragment ions. Nearly all mass spectrometers discriminate against fragment ions because their kinetic energy leads to incomplete extraction and collection. Individual mass spectrometers must be carefully characterized as to the degree of fragment ion discrimination before this absolute cracking pattern can be properly utilized.

Measurements of the threshold region for formation of the Si^+ fragment were made on three separate occasions over a span of 8 months, each measurement being the sum of four or more independent runs representing a total of over 8 h of signal accumulation. Figure 7(a) shows one such measurement. The solid line represents the Rydberg ionization function of the form $\ln E/E$ which was fit to the data below 9 eV. Figure 7(b) shows the threshold for $\text{SiF} \rightarrow \text{Si}^+$ after subtraction of this Rydberg function from the data and addition of the values of each set of three adjacent data points. Although there is considerable noise, all three measurements revealed the same three features, within the stated uncertainties.

The most prominent threshold at 14.3 ± 1.0 eV corresponds to dissociative ionization, $\text{SiF} + e^- \rightarrow \text{Si}^+ + \text{F} + 2e^-$. This process has a 13.8 ± 0.26 eV dissociation limit (the uncertainty being dominated by the uncertain bond energy, 5.68 ± 0.26 eV¹⁴). The highest observed break at 17.0 ± 1.0 eV is less prominent, but seems to be reproducible. It lies above only one dissociative ionization limit, the lowest one at 13.8 eV, and above two ion pair limits (Fig. 8). The energy difference would lead to the release of a relatively

TABLE II. Measured absolute cross section and ratio values at 70 eV.

	Measured absolute cross section (Å²)	Cross section ratio
$\text{SiF} + e^- \rightarrow \text{SiF}^+ + 2e^-$	3.90 ± 0.32^a	
Si^+/SiF^+		0.528 ± 0.024^a
F^+/SiF^+		0.060 ± 0.008

^a Average of seven measurements.

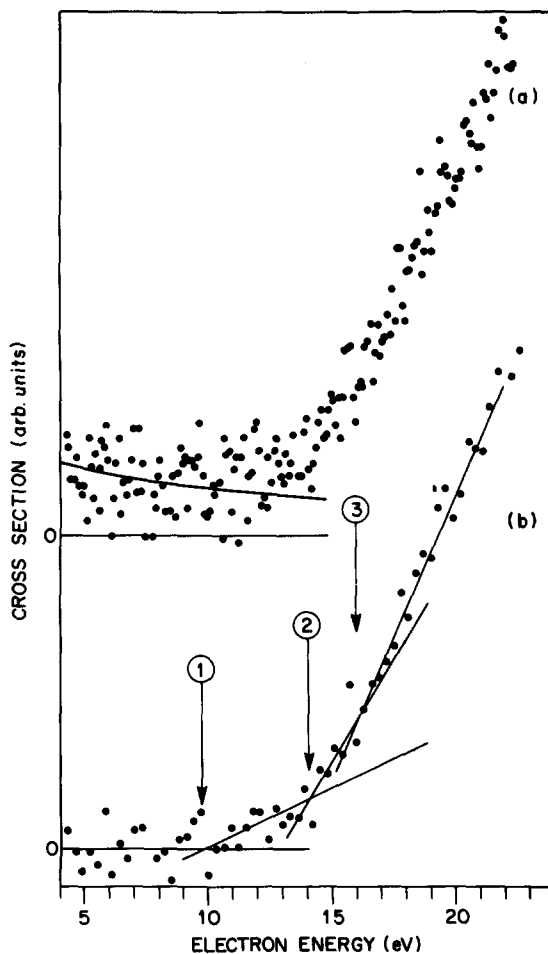


FIG. 7. Threshold region for the appearance of Si^+ from SiF . (a) Raw data including the background from Si Rydberg ionization. (b) Si^+ threshold after subtraction of Rydberg contribution (see the text), with each set of three adjacent points added together to improve signal-to-noise.

large amount of translational energy, consistent with the fragment kinetic energy inferred from the results in Fig. 3(a).

All three measurements show evidence of Si^+ formation below the lowest dissociative ionization threshold at 14.3 eV. Extensive efforts to extract a meaningful threshold from these data give a value of 9.9 ± 1.0 eV, over 3 eV below the thermochemical dissociative ionization limit. We consider three possible explanations for this surprisingly low threshold. Dissociative ionization from vibrationally excited SiF radicals can be ruled out because they would need over 3 eV of vibrational excitation, but Fig. 5 reveals that they have no more than 1 eV of vibrational excitation, and only a small fraction of them has that much. A second explanation rests on the assumption of "impurity" neutral silicon atoms being present in the beam, formed by collisional dissociation in the charge transfer cell. This explanation can also be ruled out in the following ways. Collisional dissociation is expected to produce fragments with a larger angular spread than charge transfer, so improved beam collimation should discriminate against these fragments. Our first measurement of the Si^+ threshold was made with the charge transfer cell in the middle vacuum chamber while a recent change moved it to the first chamber, just after the velocity filter. This change re-

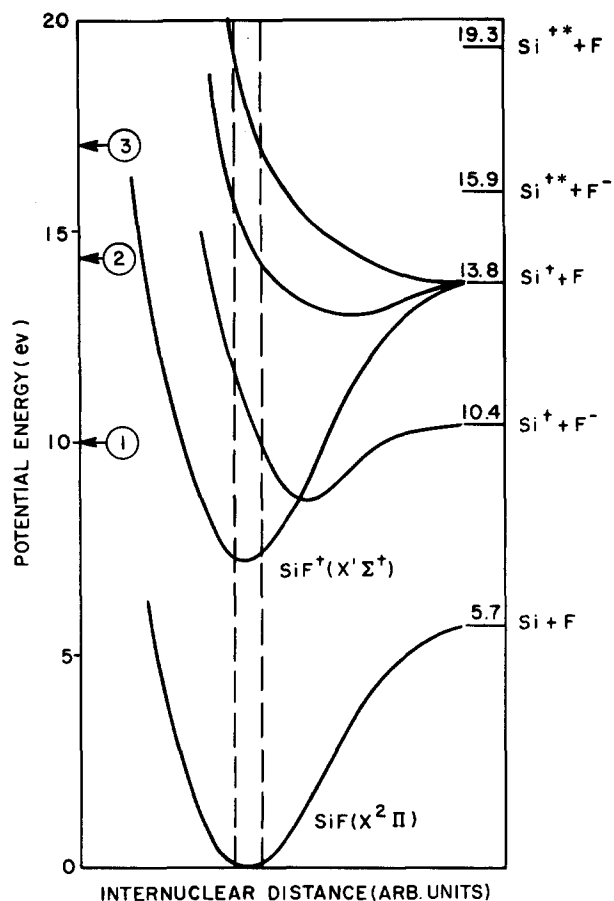


FIG. 8. Schematic potential energy diagram for SiF. The circled 1, 2, and 3 indicate the measured Si^+ thresholds.

duces the solid angle of the accepted beam by a factor of 4, yet the signal intensity between 9.9 and 14.3 eV did not change noticeably. As an additional argument, the observed threshold appears to be about 2 eV above the 8.15 eV ionization potential of Si, significantly outside the estimated uncertainty.

We conclude, therefore, that a third explanation, ion pair production, is responsible for the Si^+ signal below 14.3 eV. Because the fluorine atom has a 3.4 eV electron affinity,¹⁵ the ion pair threshold is 10.4 ± 0.26 eV, in agreement with the measured value. The energy of the peak and the magnitude of the ion pair cross section at its peak cannot be determined from the data, but the extrapolated slope from the threshold region suggests that the peak cross section might be quite large, of order 10^{-17} cm². Ion pair formation is well known in studies of ionization.¹⁶ The large cross section, one suspects, is in some way related to the large electron affinity of the fluorine atom. A considerable effort was made to observe the negative ion directly, but it was unsuccessful. The reasons, we believe, are experimental: There was a large background of F^- from collisional dissociative ionization of

the neutral SiF beam. In addition, the CEM detects F^- inefficiently because the entrance cone must be negative with respect to its output, and this retards incoming negative ions. Attempts to float the CEM at a positive potential did not produce a signal and led to the destruction of the CEM and the termination of the attempt to observe F^- .

The lowest dissociation limit leading to F^+ is calculated to be at 23.1 eV. Due to the low signal-to-noise ratio for the F^+ cross section, and weakness of the signal at threshold, we are unable to measure a meaningful threshold.

IV. CONCLUSIONS

A beam of neutral SiF can be produced by near-resonant charge transfer between Xe and a metastable electronic state of SiF^+ . SiF forms in its ground electronic state with little vibrational energy. The most abundant ion arising from electron-impact ionization of SiF is the parent SiF^+ , with the yield of Si^+ roughly one-half, and of F^+ less than one-tenth that of the parent ion (Table I and Fig. 6). The parent ion cross section peaks near 28 eV, or about four times the ionization potential. The fragment ion cross sections peak at higher energies and less sharply than the parent ion. The shape of the Si^+ fragment ion cross section shows structure near threshold, consistent with multiple dissociation processes. Ion pair production explains the lowest Si^+ threshold, while dissociative ionization explains the major process.

ACKNOWLEDGMENT

We thank Dr. R. Shul for advice on the interpretation of the measurements.

- ¹F. A. Baiocchi, R. C. Wetzel, and R. S. Freund, *Phys. Rev. Lett.* **53**, 771 (1984).
- ²H. F. Winters and F. A. Houle, *J. Appl. Phys.* **54**, 1218 (1983); M. J. Vasile and F. A. Stevie, *ibid.* **53**, 3799 (1982).
- ³Y. Matsumi, S. Toyoda, T. Hayashi, M. Miyamura, H. Yoshikawa, and S. Komiya, *J. Appl. Phys.* **60**, 4102 (1986).
- ⁴R. Walkup, Ph. Avouris, R. W. Dreyfus, J. M. Jasinski, and G. S. Selwyn, *Appl. Phys. Lett.* **45**, 372 (1984).
- ⁵R. C. Wetzel, F. A. Baiocchi, T. R. Hayes, and R. S. Freund, *Phys. Rev. A* **35**, 559 (1987).
- ⁶Galileo Electro-Optics Corporation, model 4816A2.
- ⁷D. W. O. Heddle, *Proc. Phys. Soc.* **90**, 81 (1967).
- ⁸M. R. Spalburg, J. Los, and E. A. Gislason, *Chem. Phys.* **94**, 327 (1985).
- ⁹J. W. C. Johns and R. F. Barrow, *Proc. Phys. Soc. London* **71**, 476 (1958).
- ¹⁰K. P. Huber and G. Herzberg, *Molecular Spectra and Molecular Structure. IV. Constant of Diatomic Molecules* (Van Nostrand Reinhold, New York, 1979).
- ¹¹S. J. Davis and S. G. Hadley, *Phys. Rev. A* **14**, 1146 (1976).
- ¹²I. C. Percival and D. Richards, *Adv. At. Mol. Phys.* **11**, 1 (1975).
- ¹³S. M. Younger and T. D. Märk, in *Electron Impact Ionization*, edited by T. D. Märk and G. H. Dunn (Springer, New York, 1985), Chap. 2.
- ¹⁴R. Walsh, *J. Chem. Soc. Faraday Trans.* **79**, 2233 (1983).
- ¹⁵A. A. Christodoulides, D. C. McCorkle, and L. G. Christophorou, in *Electron-Molecule Interactions and their Applications*, edited by L. G. Christophorou (Academic, Orlando, 1984), Vol. 2.
- ¹⁶L. G. Christophorou, D. L. McCorkle, and A. A. Christodoulides, in *Ref.* **15**, pp. 491, 593.